19th Brazilian Congress of Thermal Sciences and Engineering
November 06th-10th, 2022, Bento Gonçalves - RS - Brazil

ENC-2022-0553
ANALYSIS OF A RADIANT POROUS BURNER WITH ENERGY RECOVERY SYSTEM ATTACHED USING PREMIXED METHANE AND AIR

José Alexandre de Campos
Roberto Wolf Francisco Jr.
State University of Santa Catarina, Department of Mechanical Engineering, Joinville - SC, Brazil
jose.campos@edu.udesc.br
roberto.francisco@udesc.br

Abstract. *The objective of this study is to analyze the performance of a radiant porous burner with reactants preheating by means of a heat recovery device. The main parameters evaluated will be thermal efficiency, flame stability range and emission of pollutants. The heat exchanger consists of an inox alloy tube coil installed on the side of the burner, recovering of part of the energy lost to the environment through the burner walls, preheating the air. All tests are performed using CH4 as fuel, at the same equivalence ratio of 0.50. The results obtained with the reagents supplied under standard conditions, show a stable combustion regime for flame speeds between 0.6 cm/s and 0.36 m/s. With the heat recovery system, the stable combustion region expanded to a maximum flame speed of 0.40 m/s, with higher combustion temperatures. The surface temperature presented similar values, in both cases, thus the radiation efficiency results were near the same. The radiation efficiency decreased as the flame speed increases, ranging from 20.6% in the flame speed of 0.08 m/s to 15.37% at 0.40 m/s with the reactants preheated. CO emissions decreased at higher flame speeds and with higher combustion temperatures.*

Keywords: *radiant porous burner, reactants preheating, heat recovery system.*

1. INTRODUCTION

Radiant porous burners are a promising combustion technology, which can provide combustion with low pollutant emissions levels, a wide flame stability range at lean air fuel ratios and high radiation efficiency. The main characteristics of porous media combustion is the heat recirculation effect, according to Wood and Harris (2008), this effect combines the three ways that the heat transfer occurs: conduction, convection and radiation. Barra and Ellzey (2004) comments that the presence of the porous matrix facilitate the heat transfer from the combustion region to the unburned reactants gases upstream, preheating the air fuel mixture.

In addition to heat recirculation, the presence of the porous medium improves the mixing of reactants, as demonstrated by Liu et al. (2014) in a numerical analysis of a Y-shaped mesoscale combustor. The presence of the porous medium changes the main mixing mechanism, from molecular diffusion to mass dispersion, providing a more efficient way for the combination of reactants. Gao et al (2014a) made an analysis with different materials for the porous medium: silicon carbide (SiC), alumina (Al2O3) and zirconia (ZrO2), and a metallic alloy (FeCrAl). Was observed that materials with higher thermal conductivity presents a wider flame stability range. In this study the metallic alloy foam presented better result than the ceramic materials, with SiC ceramic foam outperforming the Al2O3 and ZrO2 foams.

Sinha and Muthukumar (2019), in a recent study with different ceramic materials observed similar results, with SiC ceramic foam presenting a wider flame stability limit than the other materials. Due to the fact that material with higher thermal conductivity, enhances the heat recirculation effect by enabling the displacement of the combustion regions upstream, facilitating the reactants preheating.

In a different study Gao et al. (2014b), verified the influence of how the different forms for the porous matrix: foams, beads, honeycombs, can influence the combustion behavior of the radiant porous burner. It was verified that the foams porous matrix offers a wider stability range, meanwhile the one made with spheres achieved stability with lower input power level, with the porous matrix with honeycombs offering the thinnest stability range. Heat transfer from the combustion region to the preheat zone is important for the flame stability of the radiant porous burner, with foam porous media having a wider flame stability region. This can be explained due to a more effective heat recirculation effect due to a more complex path that the reactants must traverse before reaching the combustion region.

For the pollutant emissions, different aspects of the radiant porous burner operation conditions, can influence its emissions levels, as the type of fuel, porous matrix type and material. Devi et al (2017), comments that the equivalence ratio and input power are correlated with carbon monoxide (CO) and nitrous oxide (NO_x) emissions. Emissions of these pollutants grow with the increase in the equivalence ratio. Habib et al. (2021), analyzed the combustion of biogas and CH4, and was able to verify that as the flame speed increases there is a reduction on the CO emission. CO emissions are affected by the combustion reaction temperature, where lower temperatures enable a rise in CO emissions. which lead to the combustion of biogas having a higher emission level of CO. Maznoy et al. (2018), mention that the oxidation of CO into CO2 is favored at higher temperatures, and the NOx emission is more affected by the equivalence ratio.

Reactants preheating analysis were conduct by Song et al. (2017), Vandadi et al. (2013) and Wang et al (2019) It were observed that the preheating of the reactants expand the stable operation range of the radiant porous burner, making possible to achieve a stable combustion at leaner air fuel mixtures (Vandadi et al., 2013, Wang et al., 2019) and with very low calorific value fuels.

Campos and Francisco (2021) conducted tests with a radiant porous burner, preheating the air fuel mixture to a temperature of 60.0 °C, using CH_4 and a simulated biogas fuel mixture composed of 72.5% CH_4 and 27.5 % CO_2. Was observed that the preheating of the air fuel mixture expanded the upper stable combustion region, from a max flame speed of 0.44 m/s, for the reactants at ambient temperature, to 0.56 m/s with the preheating. The lower flame speed limit was the same for all conditions tested. Another aspect observed was higher temperatures near the burner injection plate for the preheated simulated biogas, with higher values than the CH_4 at ambient temperature for all the conditions tested. For the radiation efficiency, Campos and Francisco (2021) noted higher values of radiation efficiency for the lower flame speed conditions. This behavior was similar to other studies presented on the literature, as in the works from, Keramiotis et al. (2015) and Devi et al (2017), attributing this reduction on efficiency as the flame speed grows to higher energy losses to the environment at higher flame speeds. And a lower residence time inside the burner for the combustion reaction products, limiting heat transfer from burned gases to the porous matrix. Overall, the preheated biogas presented higher efficiency levels than the fuels tested at ambient temperature.

Banerjee and Paul (2021) in a recent review listed different applications for the porous media combustion technologies, as hydrogen and syngas synthesis, low calorific values fuels, heat exchangers, heavy oil and gas extraction, food industries, and others. And concludes that are space for further research developments in areas concerning, fuel flexibility, modelling, and reactor development.

Considering the studies with radiant porous burners, the present work focuses on the experimental analysis of CH_4 combustion in a radiant porous burner, with a heat recovery system. The objective of this system is to recover part of the combustion energy that would be lost to the environment through the burner side walls and preheat the air before it is mixed with the fuel. The utilization of the heat recovery system can facilitate the burn of low calorific value fuel, as syngas and biogas with high CO2 content, and low equivalence ratios, without the necessity of an external heat source to preheat the reactants.

In this study, the behavior of the burner with and without the presence of the heat exchanger will be compared. The main parameters that will be studied are the radiation efficiency, the stability range and pollutant emissions.

2. EXPERIMENTAL SETUP AND METHODOLOGY

2.1 Experimental setup

Figure 1 presents the experimental setup diagram utilized on the tests, the components can be separated in three distinct groups, the first one contains the air and fuel supply system, the second is composed by the radiant porous burner and the third contains the data acquisition systems.

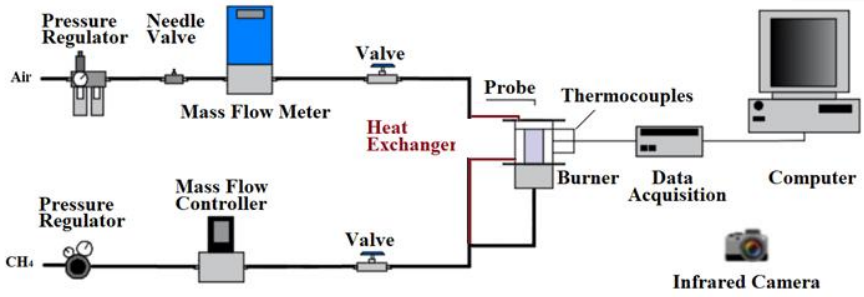

Figure 1. Experimental setup schematic.

The air supply system consists of an air compressor, a pressure regulator and coalescing filters. A needle valve was used to control the mass flow, and an OMEGA FMA-2323 mass flow meter with a maximum measurement range of 100

SLPM and a resolution of 0.1 SLPM was used for the measurement. For the fuel, was used methane gas (CH_4) with a purity of 99,5% is stored in a pressure vessel, a pressure regulator is used to reduce the pressure to 1,0 bar, and it the mass flow is regulated with an OMEGA FMA-2608A mass flow controller with a measurement range of 0 – 20 SLPM and a resolution of 0,001 SLPM.

For the tests conduct without the air preheating, the air and the CH_4 were mixed in position away from the burner inlet then feed to it through a line with 10 mm in diameter. For tests carried out with the heat exchanger, only the air is heated in the heat exchanger and then pre-mixed with the fuel, before injecting it into the burner. The heat exchanger consists of a 304 stainless steel coil tube, 6.0 mm in outer diameter, positioned inside the burner body, inserted into the layers of insulating material installed between the porous matrix and the burner housing.

The radiant porous burner used in this experiment, consists of a typical two-layer design. The first layer comprehends the preheating region – PR, which is situated upstream above the base plate, it is made of two porous mediums foams composed of SiC, with a porosity of 20 ppi, 70.0 mm in diameter and 21.5 mm high. The second layer, downstream, is the stable burning region – SBR, and is composed of three SiC porous mediums with a porosity of 10 ppi. Surrounding the porous matrixes was installed an insulating fiber inside an inox alloy case with an internal diameter of 120.0 mm as shown in Fig. 2.

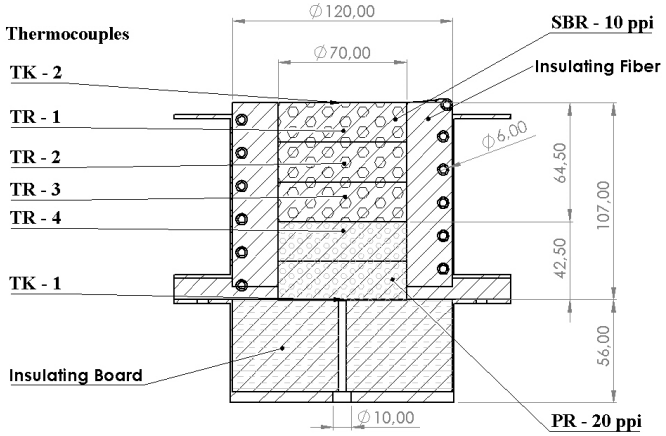

Figure 2. Radiant porous burner.

The burner temperatures were monitored by a series of thermocouples, positioned along the center axis of the burner, as indicated in Fig. 2. At base of the burner, is used a type K thermocouple, and positioned inside the porous matrix was used four type R thermocouples, for the surface another type K thermocouple was used. After the burner reached a stable operation point the surface temperature was measured by an infrared thermal camera, FLIR model T650sc. During the tests, the temperatures of the air at the inlet and outlet of the heat recovery system, the temperatures of the fuel-air mixture, and the temperature of the external surface of the burner were also measured with K-type thermocouples.

All the data collected from the thermocouples were monitored and processed utilizing a data acquisition system (Keysight DAQ970A), with the aid of the Benchvue software to monitor and record temperature readings. To calculate the input for the mass flow controllers, the Engineering Equation Solver software was used to achieve the desired equivalence ratios and flame speeds.

With all those measurements was possible determine if the radiant porous burner was operating safely, evaluate the temperatures profiles inside of the burner, visualize when the burner achieved a stable operation condition and extract the data for the analysis.

2.2 Parameter definitions

The parameters considered in the analysis are well established in the literature, as can be viewed in the studies from Francisco Jr. et al. (2010), Devi et al. (2020), and the same used by Campos and Francisco Jr. (2021).

Equation (1) presents the global combustion equation for methane gas (CH4) as a function of the equivalence ratio.

$$CH_4 + \frac{1+\phi}{\phi}(O_2 + 3.76N_2) \rightarrow CO_2 + 2\,H_2O + 7{,}52\,N_2 + \frac{1+\phi}{\phi}\,(O_2 + 3.76N_2)\,. \quad (1)$$

The equivalence ratio, ϕ, is defined as the relation between the actual fuel and air ratio provided to burner and the stoichiometric fuel and air ratio, given by Eq. (2):

$$\phi = \frac{(\dot{m}_{fuel}/\dot{m}_{air})_{ac}}{(\dot{m}_{fuel}/\dot{m}_{air})_{sto}}, \quad (2)$$

where $\dot{m}_{fuel}$ and $\dot{m}_{air}$ are the fuel mass flow rate and air mass flow rate, respectively, and the subscripts *ac* refers to the actual mass fuel ratio feed to the burner and *sto* to the stoichiometric mass fuel ratio.

Equation (3) shows the thermal power provided to the burner, S_r, and with that information is possible to determinate radiation efficiency for a given power level according to Eq. (4).

$$S_r = \dot{m}_{fuel} \cdot LHV, \quad (3)$$

$$\eta_{rad} = \frac{\varepsilon\sigma(T_{sur}^4 - T_{amb}^4)A_b}{S_r}, \quad (4)$$

where L*HV* is the fuel low heating value, η_{rad} is the radiation efficiency, ε is the emissivity of the burner, σ is Stefan-Boltzmann constant, A_b is burner surface area, *T* is the temperature with the subscripts *sur* and *amb*, referring to respectively, surface and ambient. For this study the emissivity of the burner was considered equals to 1.

Equation (5) presents the equation for uncertainty analysis, used to determinate the uncertainties related to experimental setup.

$$UM_y = \sqrt{\sum_{i=1}^{n} \left(\frac{\partial y}{\partial x_i} UM_{xi}\right)^2}, \quad (5)$$

where UM_y is the measurement uncertainty of function *y*, UM_{xi} represents the uncertainty associated to each measurement system, $\partial y/\partial x_n$ is the partial derivative of function *y* regarding x_i measurement system and *n* is the total number of measurement systems.

Table 1 presents the measurement uncertainties of the instruments used. Table 2 shows the results of uncertainty analysis calculated for the main parameters utilized in this study, thermal power and radiation efficiency.

Table 1. Measurement equipment uncertainties

Measurement Instrument	**Uncertainty**
CH4 mass flow controller FMA-2608A	± 1.0 % Full Scale
Air mass flow controller FMA-2323	± (0.8 % Reading + 0.2 % of Full Scale)
Infrared Camera – Flir T650sc	± (1.0 ºC ± 1.0% of reading)
Thermocouples	± 2.0 ºC

Table 2. Uncertainty analysis

Parameter	**Uncertainty**
Thermal load - Sr	± 54.6 [W]
Radiation efficiency - η_{rad}	± 3.31 %

For the pollutant emission, was used a TESTO 350 combustion and emissions analyzer, and on Tab. 3, is presented the chemical species, which can be analyzed, and the associate accuracy, resolution and response time for each sensor.

Table 3. Pollutant emission equipment uncertainties

Chemical Species	**Accuracy**	**Resolution**	**Response time**
O2	±0.2Vol.%	0,01 Vol. %	< 20s (t95
NO	±5ppm (0…99ppm) ±5% of reading (100…1999ppm) ±10% of reading (rest of range)	1 ppm	< 30s (t90)
NO2	±5ppm (0…99.9ppm) ±5% of reading (rest of range)	0,1 ppm	< 40s (t90)
CO	±10ppm (0…199ppm) ±5% of reading (200…2000ppm) ±10% of reading (rest of range)	1 ppm	< 40s (t90)
CO2	±0.3Vol.% ±1% of reading (0…25Vol.%) ±0.5Vol.% ±1.5% of reading (rest of range)	0,01 Vol. %	< 10s (t90) heat up time: < 15s

2.3 Experimental procedure

The experimental procedure adopted for the study is similar to one used by Campos and Francisco (2021). Initially is set up an equivalence ratio that permits the ignition of the air fuel mixture and allows the flame front to propagate into the porous matrix, heating the porous material. When the thermocouple positioned at the base of the burner reaches a temperature near to 1000 ºC, the test operating condition is applied, setting the corresponding air and fuel flow values. The temperatures are monitored constantly while the burner is under operation to verify the flame propagation behavior inside the burner. A stable point is reached when the temperatures measured along the burner exhibit an almost constant behavior over a period of 20 minutes. To avoid the degradation of the porous material, during the tests he maximum allowable operating temperature has been limited to approximately 1673 K.

(a) (b)

Figure 3. Blowout limits (a) Flame starts to move above burner surface, (b) Flame front out of the burner.

The limits of the radiant porous operation are defined as ability of the burner to operate with a stable flame, for a given set of conditions, equivalence ratio and flame speed. Outside of the stable operation region, the flame cannot sustain itself and extinguishes. The upper limit is called blow off or lift off limit, occurs when the flame detaches from the burner surface, due to the displacement of the reaction zone caused by the volumetric flow of the reactants, after this point the heat recirculation effect ceases, and this leads to the flame extinction. Figure 3 displays the moments when the flame starts to creep over the burner surface, Fig. 3a, and a few moments after, Fig. 3b, with the flame partially over the burner surface.

The lower stability limit is called flashback limit or flame quenching limit and occurs at low input power condition with low flame speed, in this situation the local flame speed is higher than the flow velocity of the unburned gases, causing the movement of the combustion zone upstream, toward the base plate of the burner, resulting in the flame extinction or the flashback. The flashback may occur when the temperature measured at the base of the burner is greater than 1100°C, which leads to the cease of the fuel flow to prevent any damage to experimental apparatus.

3. RESULTS AND DISCUSSION

In this section will be presented the results for the tests for the air fuel mixture provide to the burner at standard conditions, a reactants temperature (T_{go}) of 25.0 ºC and pressure of 1.0 atm, and with the air preheated by energy recovery system installed, in this case the reactants were preheat at temperatures ranging from 87.15 °C and 148.15 °C depending on the input power provided. All the tests were conducted with an equivalence ratio of 0.50, utilizing methane gas (CH_4) as fuel with a low heating value of 50.0 MJ/kg. Flame stability limits, temperatures profiles, radiation efficiency and pollutant emission are analyzed.

3.1 Combustion reaction limits and burner temperature profile

For Ø = 0.50 e T_{go} = 25 ºC, it was possible to obtain a flame speed range between 0.08 m/s and 0.36 m/s, corresponding to a range of thermal power (Sr) between 0.51 kW and 2.23 kW. Thermal powers of less than 0.51 kW result in a condition where the flame was not sustainable and extinguishes. Thermal powers greater than 2.23 kW resulted in flame detachment from the burner surface, reaching the blowout limit. In this case, the flow rate of the fuel-air mixture was high enough to push the flame front out of the porous matrix, in which case the heat recirculation effect ceases, and the flame is extinguished.

The preheated air, expanded the upper limit of the combustion stable region, achieving a maximum flame speed of 0.40 m/s, which corresponds to an input power of 2.53 kW, the lower stable limit remained unchanged at 0.08 m/s.

Figure 4 displays the temperatures profiles for a different flames speeds configurations covering the stable operation conditions, for the reactants at standard conditions (a), and with the heat recovery system (b). In this graph the temperatures are plotted as function of the thermocouple position and is possible to observe important aspects of the radiant porous burner operation. The first one, the temperature increase with the raise of the flame speed, as the flame speed increases more power is provided to the burner and that results in higher temperatures recorded across the burner.

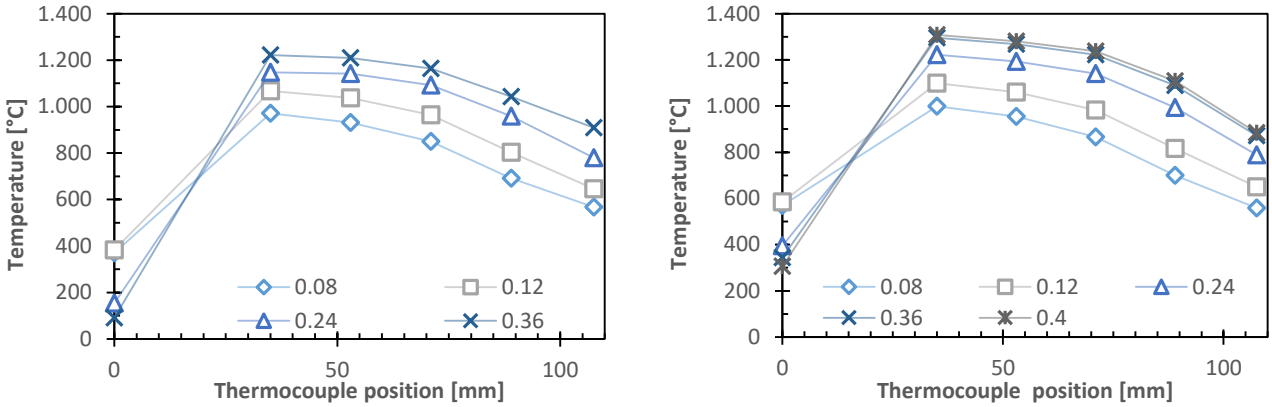

Figure 4. Temperature profiles: (a) Standard conditions, (b) with heat recovery system preheating the air.

Another aspect that can be viewed is that for all cases tested, the highest temperatures were recorded at the thermocouple positioned 35.0 mm away from the base of the burner. One possible cause for this behavior, might be due to this thermocouple be the one nearest to the interface where there the change in the porosity, from 20 ppi to 10 ppi, and according to Gao et al. (2013), this interface can act like a flame arrester, restricting the displacement of the combustion zone, forcing the combustion reaction to occur near the interface.

For the highest flames speeds, the reactants volume flow is high enough to causes the displacement of the flame front downstream. In both cases, can be observed through the temperatures recorded at the base of the burner, as the flame speed increases there is a reduction in the base temperatures, indicating a displacement of the combustion zone (position of the flame front) downstream. For the reactant gases at standard conditions (STD), the highest temperatures recorded was 1221.9 °C, for a flame speed of 0.36 m/s, at the same flame speed configuration utilizing the energy recovery system the maximum temperature at the same point was 1296.15 °C, and the maximum temperature recorded 1308.12 °C at a flame speed of 4.0 m/s.

Figure 5 shows the air temperatures at the inlet and outlet of the heat recovery system and the temperatures of the reactants before the radiant porous burner. In Fig. 5, intake represents the temperature of the air at entrance of the heat recovery system which is situated near the burner surface, and exit is the air temperature as it leaves the system near the base of the burner. With this system was possible achieve preheated air temperatures, high as 209.53 °C at a flame speed of 0.12 m/s, the lowest preheated air temperature recorded was 183.30 °C for the lowest flame speed. At higher flow rates is possible to note a decrease in air temperatures at the exit of the heat recovery system, even though the temperatures inside the burner are higher, caused by the lower residence time of the air inside the heat recovery system.

After mixing the preheated air with the CH_4 under standard conditions, the resulting temperatures for the reactants ranged from 87.15°C at 0.08 m/s to 148.15°C at 0.36 m/s. Reactant temperatures in standard condition are indicated as reactants STD in Fig. 5.

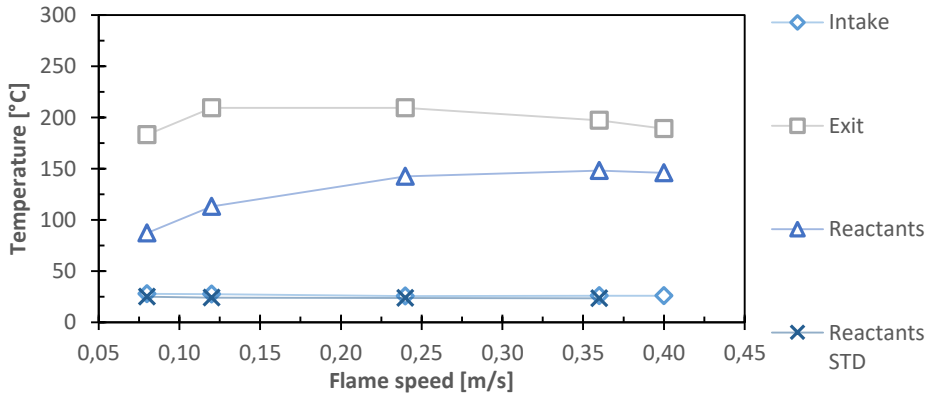

Figure 5. Air temperatures and reactants temperatures.

These higher reactants temperatures observed with the use of energy recovery system, have an impact of the temperatures profiles as seen in Fig. 4, with a higher reactant temperature, the combustion temperatures increase, which

increases the temperatures across the length of the burner, with temperature gains ranging from 1.15 to 2.85% for the lowest flame speed and gains from 4.3 to 6.07% for the 0.36 m/s flame speed. At the base of burner, was observed temperatures 200 °C higher, in average. Resulting in gains ranging from 53.86% for a flame speed of 0.08 m/s and at a temperature almost 3 times higher at 0.36 m/s, with the use of the heat recovery system.

During the tests, the side surface burner was also monitored at the points corresponding to the thermocouple Tr-2 and Tr-4, positioned at 35 and 71 mm respectively from the burner base. With the use of the heat recovery system, a significant reduction in the temperatures of the external wall of the burner was observed. The highest temperature recorded on the side surface of the burner was 251.4 °C for a flame speed of 0.36 m/s. With the energy recovery system, the highest temperature recorded was 170.02 °C for a flame speed of 0.12 m/s, at higher flames speed the temperature at burner lateral surface reduced.

3.2 Surface temperature and radiation efficiency

The surface temperature is important to calculate the radiation efficiency, as demonstrated by Eq. (4). Figure 6 shows the behavior of surface temperature as a function of flame speed. It is possible to see that the increase in the flame speed results in an increase in the surface temperature, due to the greater thermal power applied to the burner.

At the surface of the burner the use heat recovery system on its current configuration, caused a 4.0% reduction on the burner surface at higher flames speeds, as shown in Fig. 6. This can be explained due to the cold air entering the system near the burner surface, thus enhancing surface heat loss, affecting its temperature and radiation efficiencies. At intermediate flame speeds, the surface temperatures recorded were higher with the heat recovery system.

Furthermore, it is also noted that the increase in surface temperature becomes less significant as the flame speed increases, for flame speeds from 0.08 m/s to 0.24 m/s there is a gain of surface temperature close to 230.0 °C, while from 0.24 m/s to 0.40 m/s, the surface temperature increases by 120°C. According to Gao et al. (2014), this can be attributed to a greater heat loss to the environment at higher flame speeds.

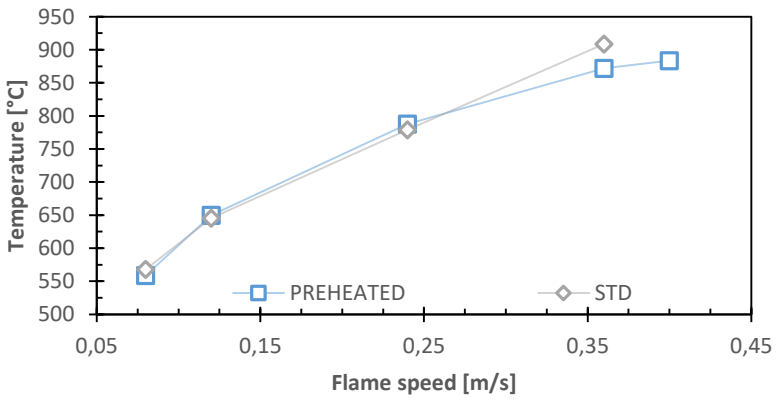

Figure 6. Surface temperatures vs. flame speed.

These temperatures were measured utilizing an infrared thermal camera, as can be viewed in Fig. 7, the thermal imaging of the radiant porous burner surface, operating with the energy recovery system, preheating the reactants.

(a) (b)

Figure 7. Surface temperatures for different flame speeds, (a) 0.08 m/s (b) 0.40 m/s.

Figure 8 show the radiation efficiency as a function of flame speed. The results obtained present a similar behavior to other studies presented on the literature, where the highest radiation efficiency is achieved at lower flame speed, and as the flame speed grows, there is a reduction on the radiation efficiency. Highest radiation efficiency obtained was

21.25% at a flame speed of 0.08 m/s for the burner without the heat recovery system, and at the maximum flame speed of 0.40 m/s achieved a radiation efficiency of 18.6%. The tests with the heat recovery system presented similar results with the intermediate flame speeds presenting higher efficiency values than the results for the reactant at standard conditions. The radiation efficiency value obtained range from 20,64% at a flame speed of 0.12 m/s to a minimal value of 15.37% for a flame speed of 0.40 m/s.

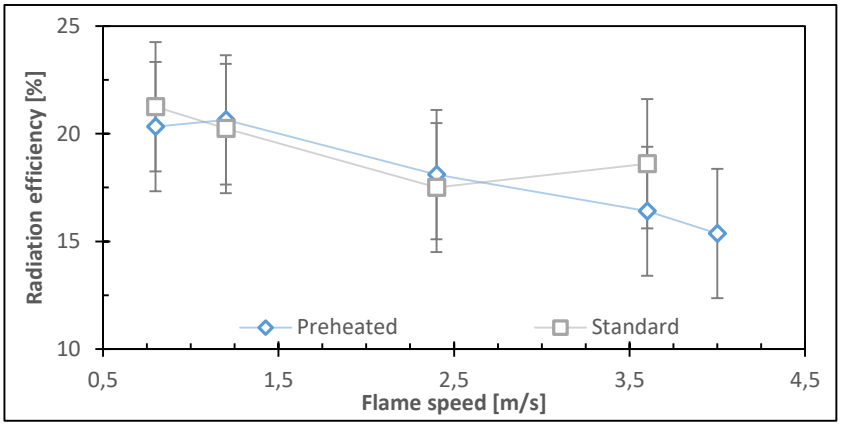

Figure 8. Radiation efficiency vs. flame speed.

Keramiotis et al. (2015) observed an increase in the radiation efficiency with the reduction of input power, attributing that to an increase in the convective heat transfer as the reactants volume flow rates increase with increments on the flame speed. Devi et al. (2020) comments that at lower flame speed, the input power provided to the burner is lower, therefore the temperatures measured at these conditions are reduced, which reduces the heat losses to the burner to the environment and make the burner able to achieve higher efficiency levels at low flame speeds.

As the flame speed increases, there is a decrease in radiation efficiency levels, and according to Arrieta et al. (2017), this efficiency behavior can be attributed to the increase in mass flow, which results in higher flow velocities for the gas phase inside the burner. Therefore, a shorter residence time of the gases within the porous matrix, limiting the heat transfer from the gas phase to the solid phase. Thus, although the surface temperature increases with increasing flame speed, these temperatures are not high enough to provide an increase in radiation efficiency for the radiant porous burner operating under these conditions.

The radiation efficiencies obtained with and without preheating the reactants are within the uncertainty range of the experiment, around 3%. Increasing the temperature of the reactants with the heat exchanger did not result in an increase in radiation efficiency, due to the lower temperature of the porous medium between the reaction zone and the burner outlet surface. This temperature reduction is the result of energy transfer to the heat exchanger, and this effect can be seen in Figs. 6 and 8.

4. POLLUTANT EMISSION

In this section, are presented the results of the CO emissions for the burner. The results obtained are shown in Fig. 9, with the emission index plotted as a function of the flame speed. For the CO emissions, is possible to observe a reduction of the CO emission index with the increase in the flame speed. Arrieta et al. (2017), Gao et al. (2012) and Maznoy et al. (2018) obtained results with similar behavior.

Higher flames speed, achieve higher reaction temperatures due to the input power increase, enable the reduction of the CO emission. Gao et al. (2012) and Song et al. (2017) comments that one of the reactions that is the main source of CO, the CO_2 dissociation reaction, $CO + OH \leftrightarrow CO_2 + H$, it occurs with greater speed at higher temperatures, which increases the consumption of CO, reducing its emissions.

For the minimal flame speed, 0,08 m/s, the emission index registered a value of 0,106 g/kg for the preheated air and 0.11 g/kg for the reactant at standard conditions, while at a flame speed of 0,36 m/s, the emission index for the standard conditions was 0.003 g/Kg, preheating the reactants reduced the emission index to 0.0013. The minimal CO emission index occurs at 0.40 m/s with a value of 0.00034 g/kg.

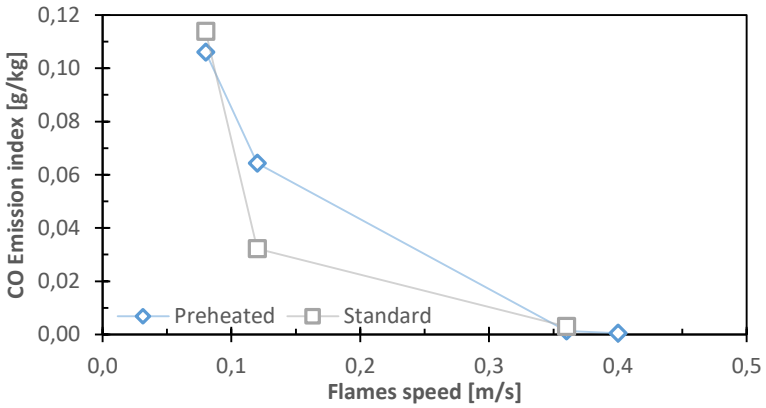

Figure 9. Pollutant emissions: CO emission index.

5. CONCLUSION

Radiant porous burners are a versatile type of burner which can operate under a different assortment of conditions. The heat recirculation effect allows the radiant porous burner to achieve a stable flame condition with very lean air fuel mixtures and makes possible the use of low calorific value fuels efficiently.

In the tests conducted, with methane gas (CH_4) at standard conditions, the radiant porous burner operated in stable combustion regime, with flame speeds ranging from 0.08 m/s to 0.36 m/s. The presence of the heat recovery system enabled the preheating of the reactants. The reactant temperatures ranged from 87.15°C for the flame speed of 0.08 m/s to maximum temperature of 148.15 °C at 0.36 m/s, with the reactants preheated the lower flame stability limit remained unchanged, at 0.08 m/s, but the lift off limit increased to a flame speed of 0.40 m/s.

The use of the heat recovery system, to preheat the air, raised the reactants temperatures, and enabled higher combustion zone temperatures for the same fuel flow conditions. The difference in the temperatures profiles was more prominent at higher flames speeds, with the greater difference in temperatures recorded at the base of the burner.

The radiation efficiency results presented a similar behavior observed in other studies, with the higher efficiency values obtained at lower flames speeds, decreasing as the flame speeds are increased. The use of the heat recovery device in the current configuration resulted in lower temperatures at the burner surface, impacting the radiation efficiency, although the obtained results are within the uncertainty range of the experiment.

For the pollutant emissions was observed a reduction on the CO emissions with the increase in the flame speed, mainly because of the higher temperatures obtained with higher input power levels.

However, the increase in the temperatures of the reaction zone, as discussed above, may allow the use of fuels with at lower equivalence ratios, leaner air fuel mixtures. Further improvements in the burner heat recovery system and isolation will conduct in order to find way to improve its performance. This study with this burner will continue in the future, evaluating low calorific value gas fuels, as syngas and biogas with high CO_2 content with distinct compositions at different equivalence ratios.

6. ACKNOWLEDGEMENTS

The authors acknowledge the financial support of the Santa Catarina State Research and Innovation Foundation (FAPESC/Brazil - grant numbers 2021TR1321, 2021TR1457 and 2021TR843), National Council for Scientific and Technological Development (CNPq/Brazil - grant number 427885/2018-3) and Coordination for the Improvement of Higher Education Personnel (CAPES - Finance Code 001).

7. REFERENCES

Arrieta, C. E., García, A. M., & Amell, A. A., 2017. "Experimental study of the combustion of natural gas and high-hydrogen content syngases in a radiant porous media burner". *International Journal of Hydrogen Energy*, 42(17), 12669–12680. https://doi.org/10.1016/j.ijhydene.2017.03.078

Banerjee, A. and Paul, D., 2021 "Developments and applications of porous medium combustion: A recent review". *Energy*, v. 221, p. 119868. Disponível em: <https://doi.org/10.1016/j.energy.2021.119868>.

Barra, A. J. e Ellzey, J. L., 2004 "Heat recirculation and heat transfer in porous burners". *Combustion and Flame*, v. 137, n. 1–2, p. 230–241.

Campos, J.A., Francisco Jr., R.W., 2021. “Effect of the carbon dioxide concentration and the preheating of the reactants on the combustion of low calorific value biogas mixtures”. *In Proceedings of the 26th International Congress of Mechanical Engineering - COBEM 2021*. Virtual congress, Brasil.

Devi, S., Sahoo, N., & Muthukumar, P., 2020. “Experimental studies on biogas combustion in a novel double layer inert Porous Radiant Burner”. *Renewable Energy*, 149, 1040–1052. https://doi.org/10.1016/j.renene.2019.10.092

Francisco Jr. R. W., Rua, F., Costa, M., Catapan, R. C., & Oliveira, A. A. M., 2010. “On the Combustion of Hydrogen-Rich Gaseous Fuels with Low Calorific Value in a Porous Burner”. *Energy and Fuels*, v. 24, n. 2, p. 880–887. https://doi.org/10.1021/ef9010324

Gao, H. Bin, Qu, Z. G., Tao, W. Q., & He, Y. L., 2012. “Experimental study of combustion in a double-layer burner packed with alumina pellets of different diameters”. *Applied Energy*, v. 100, p. 295–302, 2012. Disponível em: <http://dx.doi.org/10.1016/j.apenergy.2012.05.019>.

Gao, H. Bin, Qu, Z. G., Tao, W. Q., & He, Y. L., 2013. “Experimental investigation of methane/(Ar, N 2, CO 2)-air mixture combustion in a two-layer packed bed burner”. *Experimental Thermal and Fluid Science*, 44(x), 599–606 <https://doi.org/10.1016/j.expthermflusci.2012.08.023>.

Gao, H. B., Qu, Z.G., Feng, X.B.,Tao, W.Q., 2014a. “Methane/air premixed combustion in a two-layer porous burner with different foam materials”. *Fuel*, v. 115, p. 154–161.

Gao, H. B., Qu, Z.G., Feng, X.B.,Tao, W.Q., 2014b. “Combustion of methane/air mixtures in a two-layer porous burner: A comparison of alumina foams, beads, and honeycombs”. *Experimental Thermal and Fluid Science*, v. 52, p. 215–220, 2014 <http://dx.doi.org/10.1016/j.expthermflusci.2013.09.013>.

Habib, R., Yadollahi, B., Saeed, A., Doranehgard, M. H., Li, L.K.B., Karimi, N., 2021. “Unsteady ultra-lean combustion of methane and biogas in a porous burner – An experimental study”. *Applied Thermal Engineering*, v. 182, n. September 2020, p. 116099 <https://doi.org/10.1016/j.applthermaleng.2020.116099>.

Hashemi, S. M., and Hashemi, S. A., 2017. “Flame stability analysis of the premixed methane-air combustion in a two-layer porous media burner by numerical simulation”. *Fuel*, 202, 56–65 <https://doi.org/10.1016/j.fuel.2017.04.008>.

Keramiotis, C., Katoufa, M., Vourliotakis, G., Hatziapostolou, A., & Founti, M. A., 2015. “Experimental investigation of a radiant porous burner performance with simulated natural gas, biogas and synthesis gas fuel blends”. *Fuel*, v. 158, p. 835–842 <http://dx.doi.org/10.1016/j.fuel.2015.06.041>.

Liu, Y., Zhang, J., Wan J., Yao H. Liu, W., 2014. “Numerical investigation of CH4/O2 mixing in Y-shaped mesoscale combustors with/without porous media”. *Chemical Engineering and Processing: Process Intensification*, v. 79, p. 7–13 <http://dx.doi.org/10.1016/j.cep.2014.03.002>.

Maznoy, A., Kirdyashkin, A.,Minaev, S., Markov, A., Pichugin, N. Yakolev, E., 2018. “A study on the effects of porous structure on the environmental and radiative characteristics of cylindrical Ni-Al burners”. *Energy*, v. 160, n. X, p. 399–409 <https://doi.org/10.1016/j.energy.2018.07.017>.

Mujeebu, M. A., Abdullah, M. Z., Bakar, M. Z. A., Mohamad, A. A., & Abdullah, M. K. 2009. “Applications of porous media combustion technology - A review”. *Applied Energy*, 86(9), 1365–1375 <https://doi.org/10.1016/j.apenergy.2009.01.017>.

Song, F., Wen, Z., Dong, Z., Wang, E., & Liu, X., 2017. “Ultra-low calorific gas combustion in a gradually-varied porous burner with annular heat recirculation”. *Energy*, 119, 497–503 <https://doi.org/10.1016/j.energy.2016.12.077>.

Sinha, G. S. and Muthukumar, P., 2019. “Material characterization role in porous media combustion stability and performance”. *Materials Today: Proceedings*, v. 18, p. 5063–5068.

Vandadi, V., Park, C., and Kaviany, M., 2013. “Superadiabatic radiant porous burner with preheater and radiation corridors”. *International Journal of Heat and Mass Transfer*, v. 64, p. 680–688 <http://dx.doi.org/10.1016/j.ijheatmasstransfer.2013.04.054>.

Wang, G., Tang, P., Li, Y., Xu, J., and Durst, F., 2019. Flame front stability of low calorific fuel gas combustion with preheated air in a porous burner. Energy, 170, 1279–1288.

Wood, S. and Harris, A. T., 2008. “Porous burners for lean-burn applications”. *Progress in Energy and Combustion Science*, v. 34, n. 5, p. 667–684.

8. RESPONSIBILITY NOTICE

The authors are the only responsible for the printed material included in this paper